2022 IEEE 25th International Conference on Intelligent Transportation Systems (ITSC)
October 8-12, 2022, Macau, China

A Unified Trajectory Planning and Tracking Control Framework for Autonomous Overtaking Based on Hierarchical MPC*

Zhuoren Li[1], Lu Xiong[1] and Bo Leng[1]

2022 IEEE 25th International Conference on Intelligent Transportation Systems (ITSC) | 978-1-6654-6880-0/22/$31.00 ©2022 IEEE | DOI: 10.1109/ITSC55140.2022.9922186

Abstract— **In this paper, we develop a unified trajectory planning and tracking control framework for autonomous overtaking in structured roads. The framework consists of two individual MPC to optimize the lateral and longitudinal motion in two successive steps. The lateral MPC use the vehicle kinematic model in Frenét coordinate frame as prediction model, which is expert in describing motion in curved roads over kinematic model in Cartesian. By reformulating the MPC as a quadratic program (QP) problem, the lateral planning controller calculates the optimal steering angle control command to manage lane keeping and lane changing behaviors. Then the longitudinal planning controller will choose the mode of speed keeping or target following in accordance with the lateral result and generate the safety corridor based on ST-Graph for collision avoidance. Eventually the optimal acceleration will be given by longitudinal MPC. The hierarchical structure reduces the complexity of optimization problems and improves the efficiency for overtaking planning and control. In simulation, we use two scenarios to validate the proposed autonomous overtaking framework. The result shows the framework can deal with different overtaking maneuvers well.**

I. INTRODUCTION

In the past few decades, autonomous driving has attracted considerable interests from academic research and industrial application. Autonomous vehicles show their great potential in reducing the traffic jams and accidents. However, the scenarios that autonomous vehicles face with are always complicated, which put forward higher requirements for the trajectory planning and tracking control system. These two modules have a direct influence on vehicle's motion states, so reliable planning and control systems are the important guarantee to the safety of the vehicle.

As a complex driving task, autonomous overtaking involves both longitudinal and lateral motion planning and control. In this process, vehicles are expected to dynamically avoid the collision and choose the appropriate time to drive into the corresponding lane. Generally, an overtaking action can be regarded as three sub-actions: changing to overtaking lane, passing the front vehicle, and changing back to original lane [1]. Note that overtaking is difficult to be standardized because of the uniqueness of each real-world overtaking action, which arises from duration of overtaking, relative speed and distance between the ego vehicle and concerned vehicles, etc [2][3]. Therefore, performing an autonomous overtaking action relies on ego locations, surrounding environments and traffic conditions given by localization, perception and prediction modules along with the sophisticated planning and control systems [4].

We focus on the trajectory planning and tracking control methods for autonomous overtaking in this paper. Numerous novel algorithms and techniques have appeared in this field in the research of recent years. On the basis of traditional planning methods such as RRT and Hybrid A* [5], and widely-used control strategies such as PID and Stanley control [6], researchers made efforts to find a more efficient and suitable framework to handle autonomous overtaking maneuvers. Dixit et al. [7] developed a trajectory planning approach for high-speed overtaking based on MPC and tracked the planned overtaking trajectory by another MPC controller. And in their following research [8], a robust MPC was applied to realize the overtaking maneuver under the variable speed. The planner was proved to have the ability to perform autonomous high-speed overtaking. However, the optimal control problem in this MPC is nonlinear and the potential fields leads to a lower solve efficiency. [9] introduces a new planning framework including upper and lower planners. Upper planner models the driving environment as a resistance network to simplify the planning task and the vehicle can be modelled as a mass-point in lower planner. Consequently, two linear MPC are carried out to solve the lateral and longitudinal motion problems respectively. Lattarulo et al. [10] also uses the linear MPC and the idea of decoupling in two directions for overtaking planning. This kind of planner brings significant improvement on computational efficiency.

As we know, model predictive control has great ability to solve the multi-constrained and convex optimization problems. Therefore, most of the motion planning problems can be optimized by MPC like the research mentioned above. If we study further in these MPC-based frameworks, we will find the consistency of MPC-based planning and control. Hence the trajectory planning and tracking control tasks can be integrated into a MPC controller. This controller owns both the planning and control effects, which can unify two functions and reduce delays and errors to some extent. Rasekhipour et al. [11] and Huang et al. [12] employ the similar unified frameworks to realize the integration of motion planning and control with the artificial potential fields describing the environment. [13] also uses the unified planning and control framework to match the resistance network road model. All these algorithms optimize the final control input such as the steering angle and acceleration, perform planning and control at the same time.

Nevertheless, the general framework still has defects, such

*This work is supported by the National Natural Science Foundation of China (Grant No. 52002284) and the Science and Technology Commission of Shanghai (Grant No. 21DZ1203802).

[1]Zhuoren Li, Lu Xiong and Bo Leng are with the School of Automotive Studies, Tongji University, Shanghai, China (corresponding author: Bo Leng; e-mail: lb9161@163.com).

as lacking of capacity of planning and control in curved road. This problem can be solved with the help of Frenét coordinate frame [14]. Unlike the Cartesian coordinate frame, Frenét frame indicates object's position relative to center line or reference line no matter the line is curved or straight. In addition, the hierarchical model predictive control is also very useful to accelerate the solving process in the integrated framework.

In this paper, we propose a unified trajectory planning and tracking control framework for autonomous overtaking using hierarchical MPC. The framework employs two individual MPC controllers to solve the lateral and longitudinal motion planning and control problems respectively. We choose the vehicle kinematic model in Frenét coordinate frame as the predicted model of the ego vehicle's motion states in lateral MPC controller. This model describes the movement of the ego vehicle by the distance traveled along the lane center line and the offset distance from the lane center line. Considering the vehicle's moved distance and offset helps us simplify the motion planning problem without the loss of prediction accuracy, then the lateral planning algorithm can be formed as a linear quadratic program (QP) with collision avoidance constraints. The longitudinal planning algorithm utilize the predicted motion trajectories of surrounding obstacle vehicles provided by the motion prediction module, and the predicted trajectories which are relative to the ego vehicle's movement will be set on ST-Graph to generate a safety corridor as the constraints of longitudinal MPC. The longitudinal planning algorithm use point-mass model to form a QP problem as well. A linear optimization solver is then called to solve these optimization problems to obtain the optimal system control input.

The remaining of this paper is organized as follows. Section II introduces the vehicle kinematic model in Frenét coordinate frame used in lateral control strategy. In Section III, a linear MPC approach with constraints is used for designing the lateral planning controller. Section IV presents another linear MPC used for longitudinal controller. The constraints in longitudinal MPC are generated according to ST-Graph. This method is validated by simulation tests and the simulation results are discussed in Section V. Finally, Section VI concludes this paper.

II. VEHICLE KINEMATIC MODEL IN FRENÉT FRAME

Based on Frenét-Serret formulas, Frenét coordinate frame is established, which describes the relationship between the tangential, normal and binormal direction of the curve. Frenét frame can be used to achieve the human-like driving planning according to vehicle's movement related to the reference lines or lanes rather than the ground. Besides, local motion planning can be converted to S-L planning and S-T planning in Frenét frame. For the reason that the frame reduces the complexity of the model by decomposing a high-dimensional space planning problem into two low-dimensional space planning problems, Frenét frame is widely used in local motion planning [15][16].

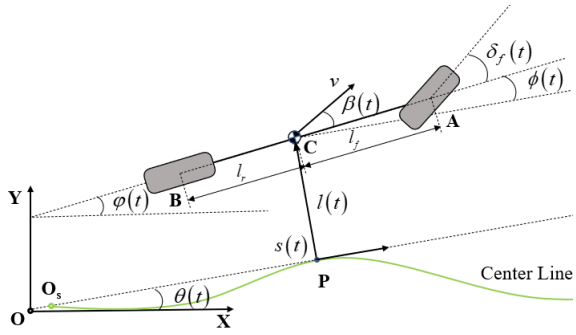

Fig. 1. Vehicle kinematic model in Frenét coordinate frame.

As shown in Fig. 1, the vehicle kinematic model in Frenét coordinate frame is given as following [17]:

$$\dot{s}(t) = \frac{v}{1-\kappa(s)l(t)} cos(\phi(t)+\beta(t)) \tag{1a}$$

$$\dot{l}(t) = vsin(\phi(t)+\beta(t)) \tag{1b}$$

$$\dot{\phi}(t) = \frac{v}{l_r} sin(\beta(t)) - \kappa(s)\dot{s}(t) \tag{1c}$$

The curvilinear abscissa $s(t)$ and the offset distance to the center line $l(t)$ indicate the position of the center of mass of the ego vehicle. The relative orientation $\phi(t)$ is defined as the difference between the heading of the ego vehicle $\varphi(t)$ and the orientation of the closest reference point on the center line $\theta(t)$. $\delta_f(t)$ represents the steering angle of the steering wheel and $\beta(t) = tan^{-1}(\frac{l_r tan\delta_f(t)}{l_f+l_r})$, where l_f and l_r are the lengths from the center of mass to the front and rear axles respectively. The center line curvature $\kappa(s)$ is related to current $s(t)$. Take into consideration that the vehicle speed v as a constant value in the lateral planning, the model has three states $\mathbf{x}(t) = [s(t), l(t), \phi(t)]^T$ and one control input $u(t) = \delta_f(t)$. (1) can be written as,

$$\dot{\mathbf{x}}(t) = f(\mathbf{x}(t), u(t)) \tag{2}$$

The model is a nonlinear control system, and we linearize the model at the current operating point $[\mathbf{x}_0, u_0]$. Defining $\hat{\mathbf{x}}_0(t)$ as the system states generated by using control u_0 at states $\mathbf{x}_0$, then $\hat{\mathbf{x}}_0(t)$ can be represented as

$$\dot{\hat{\mathbf{x}}}_0(t) = f(\hat{\mathbf{x}}_0(t), u_0) \tag{3a}$$

$$\hat{\mathbf{x}}_0(0) = \mathbf{x}_0 \tag{3b}$$

Taylor expansion is carried out at this operating point, and only the first order term is retained, while the higher order term is ignored:

$$\dot{\mathbf{x}} = f(\hat{\mathbf{x}}_0, u_0) + \frac{\partial f}{\partial \mathbf{x}}|_{\mathbf{x}=\mathbf{x}_0, u=u_0}(\mathbf{x}-\hat{\mathbf{x}}_0) + \frac{\partial f}{\partial u}|_{\mathbf{x}=\mathbf{x}_0, u=u_0}(u-u_0) \tag{4}$$

Then subtract (3) from (4), we have:

$$\dot{\tilde{\mathbf{x}}} = \tilde{\mathbf{A}}(t)\tilde{\mathbf{x}} + \tilde{\mathbf{B}}(t)\tilde{u} \tag{5}$$

where $\tilde{\mathbf{x}} = \mathbf{x} - \hat{\mathbf{x}}_0$, $\tilde{u} = u - u_0$, $\tilde{\mathbf{A}}(t) = \mathbf{J}_f(\mathbf{x})$, $\tilde{\mathbf{B}}(t) = \mathbf{J}_f(u)$, $\mathbf{J}_f(\mathbf{x})$ and $\mathbf{J}_f(u)$ are the Jacobian matrix of f respect to $\mathbf{x}$ and u respectively.

The following discrete-time state space equation is obtained by the discretization of continuous system (5) with sampling time T:

$$\tilde{\mathbf{x}}(k+1) = \tilde{\mathbf{A}}(k)\tilde{\mathbf{x}}(k) + \tilde{\mathbf{B}}(k)\tilde{u}(k) \tag{6}$$

where $\tilde{\mathbf{A}}(k) = \mathbf{I} + T\tilde{\mathbf{A}}(t)$, $\tilde{\mathbf{B}}(k) = T\tilde{\mathbf{B}}(t)$.

III. LATERAL PLANNING CONTROLLER

We establish the prediction model of the ego vehicle based on the model in Section II. Additionally, we define some system outputs for formulations of cost function and system constraints. The lateral planning algorithm is eventually converted to a QP problem using the basic idea of LMPC.

A. Definition of the System Output

For motion planning and control task in the structured road, we select a center line as the reference line. Vehicle should drive along this line, which means the offset distance $l(k)$ and relative orientation $\phi(k)$ are equal to zero. In this case, we choose $\mathbf{y}(k) = [l(k), \phi(k)]^T$ as the system outputs. This definition leads to the following relationship between outputs and original states,

$$\mathbf{y}(k) = \begin{bmatrix} l(k) \\ \phi(k) \end{bmatrix} = \begin{bmatrix} 0 & 1 & 0 \\ 0 & 0 & 1 \end{bmatrix} \begin{bmatrix} s(k) \\ l(k) \\ \phi(k) \end{bmatrix} = \mathbf{C}\mathbf{x}(k) \tag{8}$$

B. Cost Function

In consideration of human driving behaviors, cost function should be designed to have a good trade-off between accurate lane keeping and continuous smooth steering action. Thus, we introduce an incremental model to control and limit the control increment accurately. This approach can effectively prevent control jumps. Define state increment and control increment as:

$$\Delta\mathbf{x}(k) = \mathbf{x}(k) - \mathbf{x}(k-1) \tag{9a}$$

$$\Delta u(k) = u(k) - u(k-1) \tag{9b}$$

Introducing a new state vector $\boldsymbol{\xi}(k)$, the control incremental model can be written as:

$$\boldsymbol{\xi}(k+1) = \mathbf{A}_k\boldsymbol{\xi}(k) + \mathbf{B}_k\Delta u(k) \tag{10a}$$

$$\mathbf{y}(k) = \mathbf{C}_c\boldsymbol{\xi}(k) \tag{10b}$$

where

$$\boldsymbol{\xi}(k) = \begin{bmatrix} \Delta\mathbf{x}(k) \\ \mathbf{y}(k) \end{bmatrix}, \mathbf{A}_k = \begin{bmatrix} \tilde{\mathbf{A}}(k) & \mathbf{O}^T \\ \mathbf{C}\tilde{\mathbf{A}}(k) & \mathbf{I_2} \end{bmatrix}, \mathbf{B}_k = \begin{bmatrix} \tilde{\mathbf{B}}(k) \\ \mathbf{C}\tilde{\mathbf{B}}(k) \end{bmatrix},$$

$$\mathbf{C}_c = \begin{bmatrix} \mathbf{O} & \mathbf{I_2} \end{bmatrix}, \mathbf{O} = \begin{bmatrix} 0 & 0 & 0 \\ 0 & 0 & 0 \end{bmatrix}, \mathbf{I_2} = \begin{bmatrix} 1 & 0 \\ 0 & 1 \end{bmatrix}$$

The prediction horizon of MPC is N_p, and the control horizon is $N_c (N_p \geq N_c \geq 1)$. Then the system outputs in prediction horizon are:

$$\mathbf{Y} = \Theta\boldsymbol{\xi}(k) + \Phi\Delta\mathbf{U} \tag{11}$$

where

$$\mathbf{Y} = \begin{bmatrix} \mathbf{y}(k+1) \\ \mathbf{y}(k+2) \\ \vdots \\ \mathbf{y}(k+N_p) \end{bmatrix}, \Delta\mathbf{U} = \begin{bmatrix} \Delta u(k) \\ \Delta u(k+1) \\ \vdots \\ \Delta u(k+N_c-1) \end{bmatrix}, \Theta = \begin{bmatrix} \mathbf{C}_c\mathbf{A}_k \\ \mathbf{C}_c\mathbf{A}_{k+1}\mathbf{A}_k \\ \vdots \\ \mathbf{C}_c(\prod_{i=1}^{N_p}\mathbf{A}_{k+Np-i}) \end{bmatrix},$$

$$\Phi = \begin{bmatrix} \mathbf{C}_c\mathbf{B}_k & \mathbf{0} & \cdots & \mathbf{0} \\ \mathbf{C}_c\mathbf{A}_{k+1}\mathbf{B}_k & \mathbf{B}_{k+1} & \cdots & \mathbf{0} \\ \vdots & \vdots & \ddots & \vdots \\ \mathbf{C}_c(\prod_{j=1}^{Np}\mathbf{A}_{k+Np-j})\mathbf{B}_k & \mathbf{C}_c(\prod_{j=1}^{Np-1}\mathbf{A}_{k+Np-j})\mathbf{B}_{k+1} & \cdots & \mathbf{C}_c(\prod_{j=1}^{Np-Nc}\mathbf{A}_{k+Np-j})\mathbf{B}_{k+Nc-1} \end{bmatrix}$$

The lateral planning task aims to minimize the lateral offset deviation and orientation deviation as well as ensure the control input smoothly. To find the optimal solution satisfying these requirements, we propose the cost function in the matrix form as following:

$$J_{lat} = \mathbf{Y}^T\mathbf{Q}\mathbf{Y} + \Delta\mathbf{U}^T\mathbf{R}\Delta\mathbf{U} \tag{12}$$

where $\mathbf{Q}$ and $\mathbf{R}$ are weighting matrices for system outputs and control increments respectively.

In (12), the first term indicates the deviations between the actual motion states and reference states, and the second term indicates the variations of control input in every control step.

Combining this cost function with (11), the problem can be rewritten as a form of QP:

$$\mathbf{min}\ J_{lat} = \frac{1}{2}\Delta\mathbf{U}^T\mathbf{H}\Delta\mathbf{U} + \mathbf{q}^T\Delta\mathbf{U} \tag{13}$$

where

$$\mathbf{H} = 2(\Phi^T\mathbf{Q}\Phi + \mathbf{R}) \ , \quad \mathbf{q} = 2\Phi^T\mathbf{Q}\Theta\boldsymbol{\xi}(k)$$

C. System Constraints

In actual traffic scenarios, obstacles and surrounding traffic participants have a great influence on the ego vehicle's movement. The vehicle should avoid any possible collision to ensure safety. In order to reduce the computational complexity of collision detection, we employ a series of circles with the same radius to approximate the shape of the ego vehicle as shown in the Fig. 2. By comparing the radius of the circle with the distances between the center of the circle and obstacles, we can easily judge whether the vehicle has collision in this position. Obviously, if obstacles or other moving objects occupy the current lane for the ego vehicle's driving, the vehicle should choose another lane as a new target lane and execute lane changing action. In this process, the reference line will also be translated to the center line of the target lane.

For realizing the collision avoidance, the position of the ego vehicle is also determined by the static obstacles and moving objects. Therefore, the time-varying system constraints are required to be formulated as $l_{min}(s(t))$ and $l_{max}(s(t))$ at the time instant t. As depicted in Fig. 3, current position of the ego vehicle at the first time instant t_i is

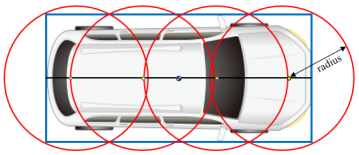

Fig. 2. Circles to approximate the vehicle shape.

$s(t_i)$. After the time interval Δt, the predicted position of the ego vehicle on reference lane center line Ω becomes $s(t_i+\Delta t)$. Meanwhile, the positions of a moving object are $(x_{obj}(t_i), y_{obj}(t_i))$ and $(x_{obj}(t_i+\Delta t), y_{obj}(t_i+\Delta t))$ at these two time instants. In this scenario, ego vehicle is white with a series of envelop circles and the moving object is red with an approximated rectangle, while the lane boundaries and static obstacles are indicated as solid lines and polygons respectively. The corresponding constraints of lateral position at these two instants are expressed as $l_{min}(s(t_i)) \le l(t_i) \le l_{max}(s(t_i))$ and $l_{min}(s(t_i+\Delta t)) \le l(t_i+\Delta t) \le l_{max}(s(t_i+\Delta t))$.

Taking the discrete system (10) into account, we can formulate the linear time-varying constraints for each future time instant k as,

$$l_{min}(s(k)) \le l(k) \le l_{max}(s(k)) \tag{14}$$

In addition to the collision avoidance constraints, we also need to restrict the system control input due to the physical limitations of the steering actuator. Besides, appropriate control increments in each step lead to a smooth driving action. Thus, we formulate corresponding constraints as

$$u_{min} \le u(k) \le u_{max} \tag{15}$$

$$\Delta u_{min} \le \Delta u(k) \le \Delta u_{max} \tag{16}$$

D. Constrained Optimal Control Problem

In order to obtain the optimal solution for (13) in whole prediction horizon, all constraints should be added on each time instant of prediction horizon and converted to the constraints of control increments $\Delta\mathbf{U}$. The original control inputs and increment constraints can be simply expressed as $\Delta\mathbf{U}_{min} = [\Delta u_{min}, \Delta u_{min}, \cdots, \Delta u_{min}]^T$, $\Delta\mathbf{U}_{max} = [\Delta u_{max}, \Delta u_{max}, \cdots, \Delta u_{max}]^T$, $\mathbf{U}_{min} = [u_{min}, u_{min}, \cdots, u_{min}]^T$, and $\mathbf{U}_{max} = [u_{max}, u_{max}, \cdots, u_{max}]^T$.

As illustrated in Section III.C, the constraints of $l(k)$ is formulated as (14), and the constraints $\phi_{min}(s(k)) \le \phi(k) \le \phi_{max}(s(k))$ should ensure the vehicle to move forward. In general, $\phi_{min}(s(k)) = -\frac{\pi}{2}$ and $\phi_{max}(s(k)) = \frac{\pi}{2}$ are regarded as the basic requirement, while the constraints of $\phi(k)$ can also be determined by specific circumstance. The definition

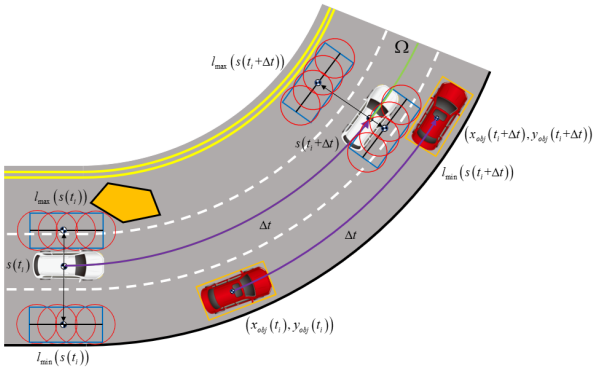

Fig. 3. The time-varying position constraints of ego vehicle at t_i and $t_i+\Delta t$.

of system output constraints are:

$$\mathbf{Y}_{min} = \begin{bmatrix} l_{min}(s(k+1)) \\ \phi_{min}(s(k+1)) \\ l_{min}(s(k+2)) \\ \phi_{min}(s(k+2)) \\ \vdots \\ l_{min}(s(k+N_p)) \\ \phi_{min}(s(k+N_p)) \end{bmatrix}, \mathbf{Y}_{max} = \begin{bmatrix} l_{max}(s(k+1)) \\ \phi_{max}(s(k+1)) \\ l_{max}(s(k+2)) \\ \phi_{max}(s(k+2)) \\ \vdots \\ l_{max}(s(k+N_p)) \\ \phi_{max}(s(k+N_p)) \end{bmatrix}$$

We use a single matrix to describe the constraints of the optimization variables $\Delta\mathbf{U}$ as

$$\mathbf{G}\Delta\mathbf{U} \le \mathbf{p} \tag{20}$$

where

$$\mathbf{G} = \begin{bmatrix} -\mathbf{I}_{N_c} \\ \mathbf{I}_{N_c} \\ -\mathbf{L}_{N_c} \\ \mathbf{L}_{N_c} \\ -\Phi \\ \Phi \end{bmatrix}, \mathbf{p} = \begin{bmatrix} -\Delta\mathbf{U}_{min} \\ \Delta\mathbf{U}_{max} \\ -\mathbf{U}_{min} + \mathbf{1}_{N_c} u(k-1) \\ \mathbf{U}_{max} - \mathbf{1}_{N_c} u(k-1) \\ -\mathbf{Y}_{min} + \Theta\boldsymbol{\xi}(k) \\ \mathbf{Y}_{max} - \Theta\boldsymbol{\xi}(k) \end{bmatrix}, \mathbf{L}_{N_c} = \begin{bmatrix} 1 & 0 & \cdots & 0 \\ 1 & 1 & \cdots & 0 \\ \vdots & \vdots & \ddots & \vdots \\ 1 & 1 & \cdots & 1 \end{bmatrix}$$

Therefore, combining cost function (13) with system constraints (20), a complete constrained quadratic optimal control problem is established as,

$$\begin{aligned} &\mathbf{min}\ J_{lat} = \tfrac{1}{2}\Delta\mathbf{U}^T\mathbf{H}\Delta\mathbf{U} + \mathbf{q}^T\Delta\mathbf{U} \\ &\mathbf{s.t.}\quad \mathbf{G}\Delta\mathbf{U} \le \mathbf{p} \end{aligned} \tag{21}$$

Taking the first control increment $\Delta u^*(k)$ of the solution $\Delta\mathbf{U}^*$ as the target control increment, the optimal control input applying to the vehicle is $u^*(k) = u(k-1) + \Delta u^*(k)$. As a result, we use LMPC to calculate the optimal steering angle $\delta^*(k)$ in each control step to accomplish the lateral motion planning and control.

IV. LONGITUDINAL PLANNING CONTROLLER

Ego vehicle's longitudinal movement is strongly influenced by the motion states of other surrounding traffic participants. Ego vehicle manages to maintain a constant speed in a driving environment without any surrounding traffic participants. However, if there are surrounding moving objects existing on the desired path for ego vehicle's driving, the vehicle should dynamically adjust the speed to avoid

collision. In this case, one of the surrounding vehicles will be selected as the target for ego vehicle to follow, which is called the preceding vehicle. And the longitudinal planning and control algorithm works as an adaptive cruise control (ACC) system [18][19] to maintain a safe distance with the preceding vehicle. In the meantime, other surrounding vehicles are all regarded as obstacle vehicles which should be avoided for safety. Therefore, we divide the longitudinal planning task into two modes: speed keeping (SK) mode and target following (TF) mode.

According to the description above, the longitudinal planning controller implement its function in three steps. The first step is to decide whether the vehicle execute the speed keeping or target following strategy and choose a reasonable target as the preceding vehicle in the latter case. The second step is generating the safety corridor by means of ST-Graph [20][21], which relies on the future motion information of obstacle vehicles. Finally, we define another LMPC problem with a quadratic cost function and linear constraints formulated by the safety corridor and solve this QP problem to achieve the longitudinal planning and control task.

A. Target Selection

When the ego vehicle fails to maintain a constant speed to drive, the longitudinal motion strategy shifts to TF mode. Then the ego vehicle should select a surrounding vehicle as target to follow and keep a safe distance with it. As a result, the longitudinal movement of the ego vehicle to some extent depends on which one the selected preceding vehicle is.

In autonomous overtaking scenario, we propose a target selection strategy with the help of the system constraints in lateral planning controller. If the unfeasible constraints of outputs arise, it is obvious that the vehicle is unable to overtake at this time instant. In this case, the ego vehicle must choose a moving object to execute target following. The future motion states of each moving objects are predicted by the motion prediction module, so we select the object in front of the ego vehicle with the highest speed as the target. If there are several objects in a same lane, we should guarantee the selection is the closest one to ego vehicle. A number of examples of selection are illustrated in Fig. 4. After following for a while, the ego vehicle will change back to SK mode and make an overtaking when no unfeasible constraint exists. In other scenarios, vehicle can also make different decisions on target selection in accordance with specific conditions.

B. Safety Corridor Generation

In case the ego vehicle is driving in TF mode, except for preceding vehicle, any other surrounding vehicles will be regarded as the obstacle vehicles. However, all of the surrounding vehicles are considered as the obstacle vehicles in SK mode. And we need to avoid the potential collisions for safe driving.

Inspired by the idea of ST-Graph in speed planning, we define the safety corridor, which represent a collision-free space for ego vehicle to drive in longitudinal direction. The generation of safety corridor are highly correlated with the

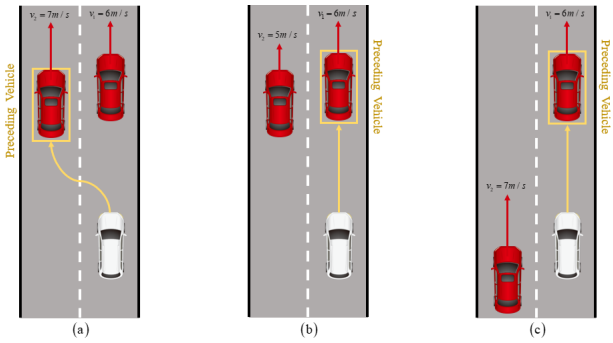

Fig. 4. Some examples of target selection.

obstacle vehicles' predicted trajectories derived from the motion prediction module. Every obstacle vehicle is indicated as a rectangle bounding box. Based on the predicted trajectories of the bounding box centers, the space occupied by bounding boxes in a future period is projected into the center line on ST-Graph, which are depicted as the red polygons in Fig. 5. Then we match these obstacle vehicles' motion states with the period when ego vehicle is possible to have a collision to determined the safety corridor. The safety corridor can be described as the blue area with in ST-Graph of Fig. 5

Overtaking can be view as the combination of two lane changing action. For this reason, we analyse the lane changing action of ego vehicle by dividing it into three phases: preparation, execution and completion as shown in Fig. 6. From lateral planning controller, we are able to get predicted states to describe the ego vehicle's positions in lane changing maneuver. The division of the three phases depends on the lateral positions p_{in} and p_{out} as well as corresponding time instants t_{in} and t_{out}. In preparation phase from 0 to t_{in}, the rectangle approximating the shape of the ego vehicle is inside the original lane, so the obstacle vehicles in original lane affect the ego vehicle's movement. In period from t_{in} to t_{out}, the ego vehicle executes lane changing action and spans two lanes. Thus the obstacle vehicles in both two lanes should be taken into consideration to bound the safety corridor. After t_{out}, the ego vehicle successfully change to the target lane, which means the whole volume of the ego vehicle is out of the original lane. Only obstacle vehicles in target lane are checked in this phase.

C. Longitudinal Motion Optimization Based on LMPC

Similar to lateral planning controller, we employ LMPC to realize the longitudinal motion optimization. However, a simple point-mass kinematic model is enough to be utilized as the prediction model. The discrete-time model with sampling time T is presented as

$$s_i(k+1) = s_i(k) + v_i(k)T + \frac{1}{2}a_i(k)T^2 \tag{22a}$$

$$v_i(k+1) = v_i(k) + a_i(k)T \tag{22b}$$

where $s_i(k)$, $v_i(k)$ and $a_i(k)$ denote the ith mass-point's distance traveled, speed and acceleration along the longitudinal direction, respectively.

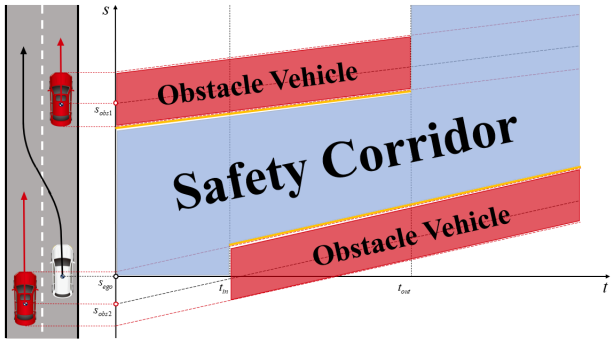

Fig. 5. The safety corridor determined by motion states of ego and obstacle vehicles in ST-Graph.

SK and TF mode put different requirements for longitudinal movement. Therefore, except for defining ego vehicle's acceleration $a_{ego}(k)$ as the same system control input, we propose different control strategies to adapt to these two modes. In SK mode, ego vehicle only need to drive inside the safety corridor at a desired speed. Hence we define the speed error between actual and desired speed $e_v(k) = v_{ego}(k) - v_d(k)$ and distance traveled in longitudinal direction $s_{ego}(k)$ as system states $\boldsymbol{\eta}(k) = [s_{ego}(k), e_v(k)]^T$. According to (22), the discrete-time state space equation of SK is:

$$\boldsymbol{\eta}(k+1) = \begin{bmatrix} 1 & T \\ 0 & 1 \end{bmatrix} \boldsymbol{\eta}(k) + \begin{bmatrix} 0.5T^2 \\ T \end{bmatrix} a_{ego}(k) \tag{23}$$

As for TF mode, we have to take the longitudinal distance from the preceding vehicle $d(k) = s_{pre}(k) - s_{ego}(k)$ into account. This distance should be maintained as our expectation $d_{exp}(k)$. Besides, the regulation of speed error between preceding and ego vehicle $v_e(k) = v_{pre}(k) - v_{ego}(k)$ also contribute to keep an expected following distance. In order to ensure the vehicle move inside the safety corridor and below the maximum speed limit in TF mode, we define the system states as $\boldsymbol{\eta}(k) = [s_{ego}(k), v_{ego}(k), d(k) - d_{exp}(k), v_e(k)]^T$ and express the discrete-time state space equation of TF as,

$$\boldsymbol{\eta}(k+1) = \begin{bmatrix} 1 & T & 0 & 0 \\ 0 & 1 & 0 & 0 \\ 0 & 0 & 1 & T \\ 0 & 0 & 0 & 1 \end{bmatrix} \boldsymbol{\eta}(k) + \begin{bmatrix} 0.5T^2 \\ T \\ -0.5T^2 \\ -T \end{bmatrix} a_{ego}(k) \tag{24}$$

The same method as in lateral planning controller is carried out to treat the model (23) and (24). We convert the original model into incremental model and define the control increment as $\Delta a_{ego}(k) = a_{ego}(k) - a_{ego}(k-1)$. It is notable that the increment of acceleration is jerk, which has a strongly influence on accelerating and braking comfort. Thus, one of longitudinal optimization objective is to minimize the jerks. In addition to this, acceleration should be optimized to make the vehicle drive at a constant speed under normal conditions. And the system states are chosen as another objective to achieve basic function of SK or TF mode. In conclusion, the cost function of longitudinal LMPC is given as,

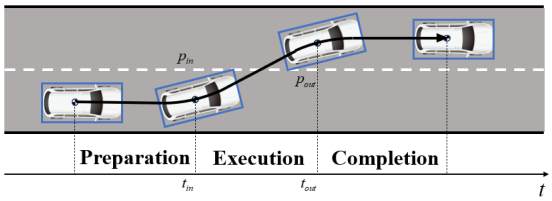

Fig. 6. Phases in lane changing: preparation, execution and completion.

$$J_{lon} = \sum_{k=1}^{N_p} \boldsymbol{\eta}(k)^T \mathbf{P} \boldsymbol{\eta}(k) + \sum_{k=0}^{N_c-1} a_{ego}(k)^T \mathbf{S_1} a_{ego}(k) + \sum_{k=0}^{N_c-1} \Delta a_{ego}(k)^T \mathbf{S_2} \Delta a_{ego}(k) \tag{25}$$

where N_p and N_c are predict horizon and control horizon same as in Section III, $\mathbf{P}$, $\mathbf{S_1}$ and $\mathbf{S_2}$ are weighting matrices for system states, control inputs and control increments, respectively. For system states $\boldsymbol{\eta}(k)$, only $d(k) - d_{exp}(k)$, $v_e(k)$ in TF mode and $e_v(k)$ in SK mode are optimization variables, so the weight of other states are zero.

Constraints should be added in (25) for collision-free and comfort movement of the ego vehicle, then we describe the longitudinal motion optimization as a complete constrained optimal control problem,

$$\begin{aligned} \textbf{min } J_{lon} = & \sum_{k=1}^{N_p} \boldsymbol{\eta}(k)^T \mathbf{P} \boldsymbol{\eta}(k) + \sum_{k=0}^{N_c-1} a_{ego}(k)^T \mathbf{S_1} a_{ego}(k) \\ & + \sum_{k=0}^{N_c-1} \Delta a_{ego}(k)^T \mathbf{S_2} \Delta a_{ego}(k) \\ \textbf{s.t.} \quad & \boldsymbol{\eta}_{min}(k) \le \boldsymbol{\eta}_{ego}(k) \le \boldsymbol{\eta}_{max}(k) \qquad k = 1, 2, \cdots, N_p \\ & a_{min}(k) \le a_{ego}(k) \le a_{max}(k) \qquad k = 0, 1, \cdots, N_c - 1 \\ & \Delta a_{min}(k) \le \Delta a_{ego}(k) \le \Delta a_{max}(k) \qquad k = 0, 1, \cdots, N_c - 1 \end{aligned} \tag{26}$$

where $(\boldsymbol{\eta}_{min}(k), \boldsymbol{\eta}_{max}(k))$ are state constraints formulated in accordance with the safety corridor and speed limit if necessary, $(a_{min}(k), a_{max}(k))$ are control input constraints, $(\Delta a_{min}(k), \Delta a_{max}(k))$ are control increment constraints.

To solve this problem, we optimize the control increments $[\Delta a_{ego}(k), \Delta a_{ego}(k+1), \cdots, \Delta a_{ego}(k+N_c-1)]^T$ by conversion based on the incremental model. The specific method can be referred to in Section III. As a result, the first optimal control input will be applied to ego vehicle as the desired longitudinal acceleration.

V. SIMULATIONS

The proposed planning and control framework is validated in the open source autonomous driving simulator CARLA [21], which provides varieties of vehicle models and driving scenes for testing. The simulation was implemented in C/C++ environment and executed on an Intel Core i7-4200 H@2.8 GHz with 8.00GB RAM. In order to solve the QP problems efficiently, we employ an open source solver OSQP [22] to perform real-time computations. We set the prediction

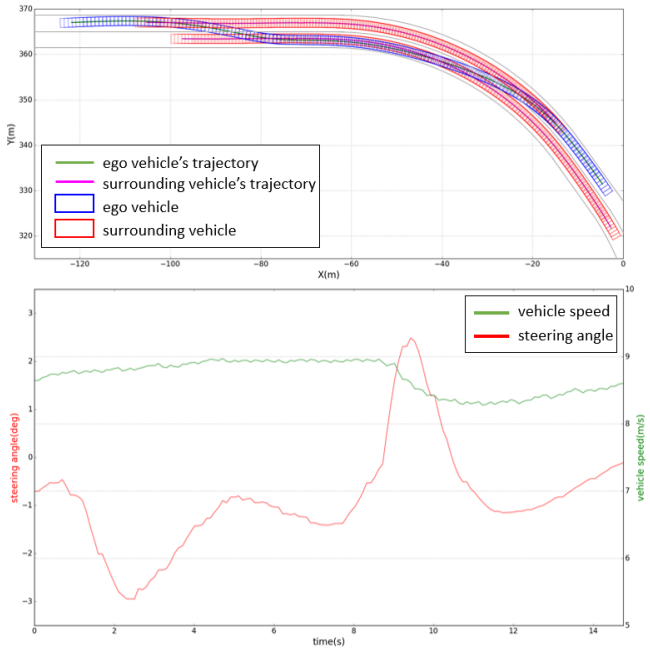

Fig. 7. The history trajectories of ego vehicle and surrounding vehicles, variation of vehicle speed and steering angle in Scenario 1.

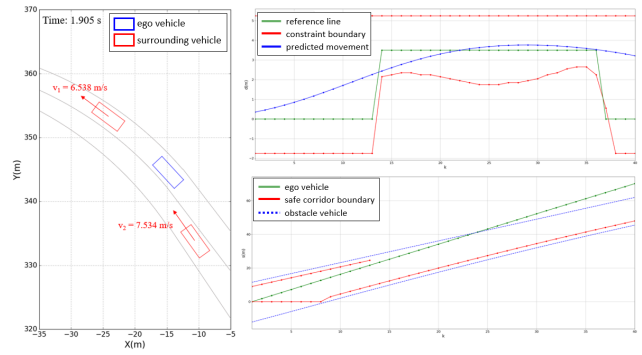

Fig. 8. Snapshot at the moment ego vehicle started to overtake and the solutions of MPC with constraints in Scenario 1.

horizon as $N_p = N_c = 40$ and the sampling step as 0.2s. $\mathbf{Q}$ and $\mathbf{R}$ in Eq.(12) are $diag\{10.0, 10.0\}$ and $diag\{5.0\}$ respectively. $\mathbf{P}$, $\mathbf{S_1}$ and $\mathbf{S_2}$ in Eq.(26) are $diag\{0.0, 0.0, 5.0, 25.0\}$, $\{1.0\}$ and $\{1.0\}$ respectively. Nevertheless the optimization time for a LMPC is no more than 5ms.

Two types of autonomous overtaking scenarios on a curved double-lane road are simulated in this section, including the immediate overtaking and overtaking after target following.

A. Scenario 1

In this scenario, a vehicle is driving in front of the ego vehicle at a lower speed $v_1 = 6.5m/s$ in current lane, while another vehicle ($v_2 = 7.5m/s$) in left lane is far behind the ego vehicle. Ego's desired speed is $v_{des} = 9.0m/s$. Under the circumstance, ego vehicle has ample space to overtake without the danger of collision.

Fig. 7 demonstrates the history trajectories moved by the ego vehicle and the surrounding vehicles as well as the

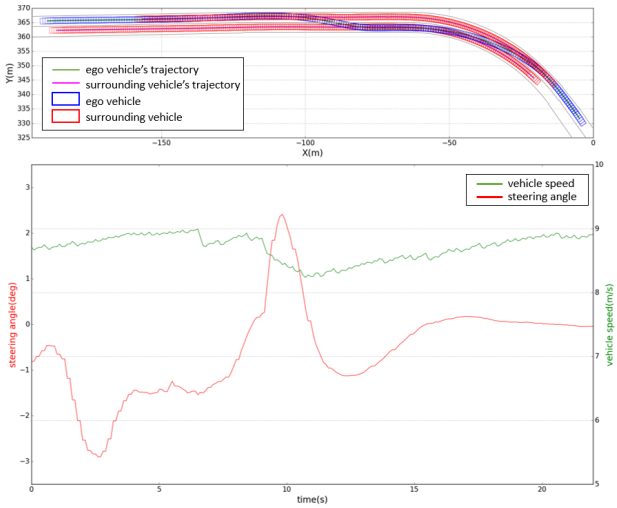

Fig. 9. The history trajectories of the ego vehicle and the surrounding vehicles, and the variation of speed and steering angle in Scenario 2.

variation of vehicle speed and steering angle of front wheel during the overtaking process. Ego Vehicle drove in speed keeping mode at all times and overtook directly. Fig.8 shows a snapshot at the moment that the ego vehicle started to overtake, when the ego vehicle would plan to drive pass the front vehicle by hierarchical lateral and longitudinal MPC.

B. Scenario 2

Unlike the scenario 1, the vehicle in left lane is in front of the ego vehicle in this scenario. The speed conditions are same as in scenario 1 ($v_1 = 6.5m/s$, $v_2 = 7.5m/s$, $v_{des} = 9.0m/s$). In this case, the ego vehicle fails to overtake immediately because the two front vehicles are too close to each other at current time. The lack of overtaking space makes the ego vehicle choose to follow the fast vehicle in left lane for some time. Then the ego vehicle completes the overtaking when there is enough clearance from the slow vehicle.

The travelled trajectories of the ego vehicle and surrounding vehicles and the all-time ego's speed and steering angle are depicted in Fig. 9. Ego vehicle entered the target following mode to follow the vehicle in left lane at first. When $t = 1.905s$, overtaking was judged as feasible, the ego vehicle switched to speed keeping mode and changed back to the original lane to finish overtaking. Fig. 10 and Fig. 11 present the snapshots in $t = 1.905s$ and $t = 9.528s$, respectively. In Fig. 11, the lateral MPC constraints indicated an infeasible problem, so the longitudinal planning controller worked in TF mode with pictured constraints. In Fig. 12, the overtaking space was not be occupied anymore, which lead to a lane changing action in SK mode of ego vehicle as the end of overtaking.

VI. CONCLUSIONS

This paper presents a unified framework of trajectory planning and tracking control for autonomous overtaking. The framework is formed by hierarchical model predictive control, which optimizes the lateral and longitudinal

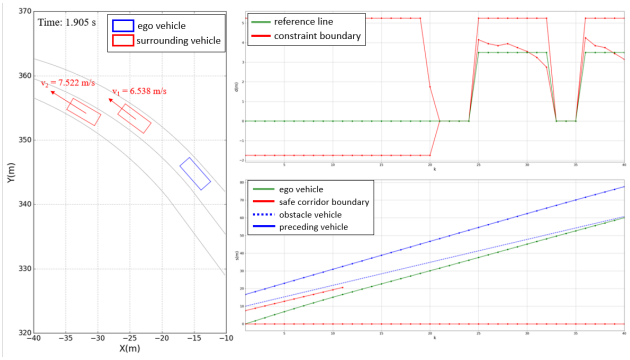

Fig. 10. Snapshot at 1.905s when ego vehicle started to following and the solutions of MPC with constraints in Scenario 2.

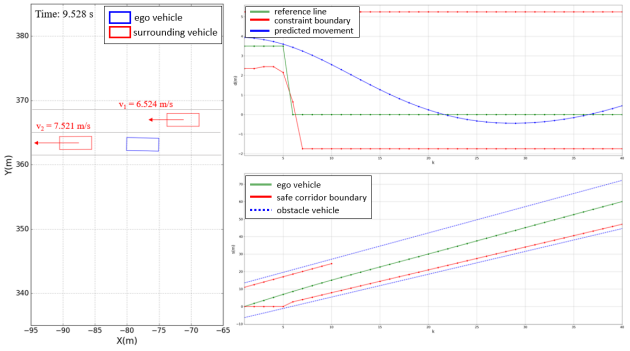

Fig. 11. Snapshot at 9.528s when ego vehicle switched mode to overtake and the solutions of MPC with constraints in Scenario 2.

movement in two successive steps. Lateral MPC controller generates the steering angle control command to manage lane keeping and lane changing behaviors. The longitudinal planning controller then selects the reasonable behavior and calculates the optimal control command in accordance with the lateral result. The hierarchical method reduces the complexity of optimization problems and improves the efficiency. We also prepared two scenarios in simulation to validate the autonomous overtaking framework. The result proves that the proposed framework is able to deal with different conditions and give the proper control commands for overtaking maneuver.

Future work will focus on considering the uncertainties of the environment. Besides, modeling by vehicle dynamic model to make the framework adapt to high-speed and critical driving situations is also worth researching.

REFERENCES

[1] P. Petrov and F. Nashashibi, "Modeling and Nonlinear Adaptive Control for Autonomous Vehicle Overtaking," *IEEE Transactions on Intelligent Transportation Systems*, vol. 15, no. 4, pp. 1643-1656, Aug. 2014.

[2] E. I. Vlahogianni, "Modeling duration of overtaking in two lane highways," *Transp. Res. F, Traffic Psychol. Behav.*, vol. 20, pp. 135–146, Sep. 2013.

[3] M. Motro, A. Chu, J. Choi et al. "Vehicular ad-hoc network simulations of overtaking maneuvers on two-lane rural highways," *Transportation Research Part C: Emerging Technologies*, vol. 72, pp. 60–76, 2016.

[4] K. Chu, M. Lee and M. Sunwoo, "Local Path Planning for Off-Road Autonomous Driving With Avoidance of Static Obstacles," *IEEE Transactions on Intelligent Transportation Systems*, vol. 13, no. 4, pp. 1599-1616, Dec. 2012.

[5] D. González, J. Pérez, V. Milanés and F. Nashashibi, "A Review of Motion Planning Techniques for Automated Vehicles," *IEEE Transactions on Intelligent Transportation Systems*, vol. 17, no. 4, pp. 1135-1145, April 2016.

[6] N. H. Amer, H. Zamzuri, K. Hudha and Z. A. Kadir, "Modelling and control strategies in path tracking control for autonomous ground vehicles: A review of state of the art and challenges", *J. Intell. Robotic Syst.*, vol. 86, no. 2, pp. 225-254, 2017.

[7] S. Dixit et al., "Trajectory planning for autonomous high-speed overtaking using MPC with terminal set constraints," in *Proc. 21st Int. Conf. Intell. Transp. Syst. (ITSC)*, Nov. 2018, pp. 1061–1068.

[8] S. Dixit et al., "Trajectory Planning for Autonomous High-Speed Overtaking in Structured Environments Using Robust MPC," *IEEE Transactions on Intelligent Transportation Systems*, vol. 21, no. 6, pp. 2310-2323, June 2020.

[9] Y. Huang, H. Wang, A. Khajepour, H. Ding, K. Yuan and Y. Qin, "A Novel Local Motion Planning Framework for Autonomous Vehicles Based on Resistance Network and Model Predictive Control," *IEEE Transactions on Vehicular Technology*, vol. 69, no. 1, pp. 55-66, Jan. 2020.

[10] R. Lattarulo, D. He and J. Pérez, "A Linear Model Predictive Planning Approach for Overtaking Manoeuvres Under Possible Collision Circumstances," *2018 IEEE Intelligent Vehicles Symposium (IV)*, Changshu, China, 2018, pp. 1340-1345.

[11] Y. Rasekhipour, A. Khajepour, S. Chen and B. Litkouhi, "A Potential Field-Based Model Predictive Path-Planning Controller for Autonomous Road Vehicles," *IEEE Transactions on Intelligent Transportation Systems*, vol. 18, no. 5, pp. 1255-1267, May 2017.

[12] Z. Huang, Q. Wu, J. Ma, and S. Fan, "An APF and MPC combined collaborative driving controller using vehicular communication technologies," *Chaos, Solitons Fractals*, vol. 89, pp. 232–242, Aug. 2016.

[13] Y. Huang et al., "A Motion Planning and Tracking Framework for Autonomous Vehicles Based on Artificial Potential Field Elaborated Resistance Network Approach,"*IEEE Transactions on Industrial Electronics*, vol. 67, no. 2, pp. 1376-1386.

[14] J. Kong, M. Pfeiffer, G. Schildbach and F. Borrelli, "Kinematic and dynamic vehicle models for autonomous driving control design," *2015 IEEE Intelligent Vehicles Symposium (IV)*, Seoul, Korea (South), 2015, pp. 1094-1099.

[15] M. Werling, S. Kammel, J. Ziegler, and L. Groll, "Optimal trajectories for time-critical street scenarios using discretized terminal manifolds," *Int. J. Robot. Res.*, vol. 31, no. 3, pp. 346–359, 2012.

[16] X. Li, Z. Sun, D. Cao, D. Liu, and H. He, "Development of a new integrated local trajectory planning and tracking control framework for autonomous ground vehicles," *Mech. Syst. Signal Process.*, vol. 87, pp. 118–137, Mar. 2017.

[17] G. Cesari, G. Schildbach, A. Carvalho and F. Borrelli, "Scenario Model Predictive Control for Lane Change Assistance and Autonomous Driving on Highways," *IEEE Intelligent Transportation Systems Magazine*, vol. 9, no. 3, pp. 23-35, Fall 2017.

[18] R. Rajamani, Vehicle Dynamics and Control. Boston, MA, USA: Springer, 2012.

[19] S. Li, K. Li, R. Rajamani, and J. Wang, "Model predictive multi-objective vehicular adaptive cruise control," *IEEE Trans. Control Syst. Technol.*, vol. 19, no. 3, pp. 556–566, May 2011.

[20] H. Li, G. Yu, B. Zhou, P. Chen, Y. Liao and D. Li, "Semantic-Level Maneuver Sampling and Trajectory Planning for On-Road Autonomous Driving in Dynamic Scenarios," *IEEE Transactions on Vehicular Technology*, vol. 70, no. 2, pp. 1122-1134, Feb. 2021.

[21] W. Lim, S. Lee, M. Sunwoo and K. Jo, "Hybrid Trajectory Planning for Autonomous Driving in On-Road Dynamic Scenarios," *IEEE Transactions on Intelligent Transportation Systems*, vol. 22, no. 1, pp. 341-355, Jan. 2021

[22] D. Alexey, R. German, C. Felipe, L. Antonio, and K. Vladlen, "CARLA: An open urban driving simulator," in *Proc. Conf.on Robot Learning (CoRL)*, pp. 445-461, Nov. 2017.

[23] B. Stellato, G. Banjac, P. Goulart, A. Bemporad and S. Boyd, "OSQP: An Operator Splitting Solver for Quadratic Programs," *2018 UKACC 12th International Conference on Control (CONTROL)*, Sheffield, UK, 2018, pp. 339-339.